Paper No. 21

ESTIMATION OF OUTGASSING FROM AN EXPENDED APOGEE MOTOR AND ITS EFFECTS ON SPACECRAFT SURFACES

John J. Scialdone, John F. Rogers, and Raymond Kruger,
Goddard Space Flight Center, Greenbelt, Maryland

ABSTRACT

An experimental and theoretical investigation has been carried out to evaluate the degradation of the solar cells and other sensitive surfaces of a spacecraft, resulting from the molecular outgassing of an expended solid propellant apogee motor. The motor, following its burnout, is retained by the spacecraft and is a source of gases and particulates which will be released mainly by the unburned propellant-to-casing insulation. The deployment of the solar array within a few minutes after the motor burn results in the interception and reflection to the surfaces of the spacecraft of the molecular outgassing and particulates. Various methods, based on some experimental data, have been used to analytically assess the magnitude of the outgassing from the engine. The results of this investigation indicate that during the 2 minutes' exposure of the solar cells to the motor outgassing, the deposit of the fraction of outgassing with low volatility on the cells will be about 6×10^{-7} g/cm^2 or about 43 Å for a material density of 1.4 g/cm^3. This is predicted on the array deployment occurring 8 minutes after motor burnout when the motor is at an average temperature of about 473 K (200°C). A solar cell degradation of less than 1 percent is predicted for this accumulation. The accretion of the same material for an indefinite time on the silver-coated Teflon insulation of the hydrazine tanks has been estimated at 5×10^{-8} g/cm^2 (3.6 Å). This thickness, according to tests, should cause no significant change in the α/ϵ of the insulation. The hydrazine tanks are exposed to a higher flux of contaminants than any other sensitive location of the spacecraft. Contaminant deposits on other spacecraft surfaces are, therefore, less than 3.6 Å and they should not be degrading.

INTRODUCTION

An experimental and theoretical investigation has been carried out to assess the probable contamination and degradation of the solar array cells and other sensitive surfaces of a spacecraft. The contamination may be produced by molecular outgassing of the spacecraft apogee motor.

A solid propellant motor is retained by the spacecraft following its firing which lasts 45 seconds and produces an impulse of about 1862 N·s (420 lb·s). The motor is a source of gases and particulates which are released mainly by the unburned propellant-to-casing insulation. The deployment of the solar array, within a few minutes after the motor burn, results in the interception and reflection toward the spacecraft surfaces of the molecular and particulate products. During a portion of the deployment sequence, a period of about 2 minutes, the solar cells surfaces of the array are exposed to the contaminant flux. After this, the other side of the array receives and reflects the contaminant toward the spacecraft. The relative position of the motor, solar paddles, and instruments on the spacecraft main body are shown in Figure 1.

The investigation is discussed in two parts: one covering an assessment of the magnitude of the contaminant deposits on the solar cells and the metal-coated Teflon insulation of the hydrazine tanks; the other, an evaluation of the effect of those deposits on the optical/thermal properties of those surfaces.

The deposit assessment portion of this report includes experimental data on the motor insulation obtained from micro-volatile condensable mass (VCM) tests, thermogravimetric tests (TG), and quartz crystal microbalance (QCM) measurements. The data are analyzed and used to generate an estimate of the magnitude of the outgassing from the motor as a function of time. These rates and other experimental data on the outgassing properties, plus view factor data, are used to estimate the deposits on the surface of interest.

EXPERIMENTAL DATA

Temperatures of the Insulation Material

Qualification tests of the solid propellant motor (Reference 1) indicate that the dome region of the titanium motor case approaches a temperature of about 523 K (250°C), at approximately 280 seconds after motor ignition. A maximum temperature of about 723 K (450°C) is measured near the nozzle 80 seconds after ignition. Many different temperatures are recorded at various locations of the case. Figure 2 shows the average temperature of the motor as a function of time. The maximum average temperature is indicated to be 506 K (233°C)

followed by a rapid drop to approximately 423 K - 413 K (150 - 140°C) in about 10 minutes.

The calculations have been based on a motor insulation temperature of 473 K (200°C) at the time of the array deployment followed by a decay of 25 K every 10 minutes. The insulation between the case and the propellant, which remains in the engine following the burn, is taken to be the source of molecular outgassing and particulates.

Insulation Material

This material is an asbestos-filled vulcanized isoprene rubber protected with other materials according to its location in the motor. The surface adjacent to the propellant is covered with an epoxy resin and carbon black in a plasticizer. The surface in contact with stagnant hot gas is coated with Teflon tape, and in another engine location, this surface is covered with a woven polypropylene industrial cloth. These sections, about equal in weight, have thicknesses between 0.5 and 1.5 mm and are cured at 355 K (82°C) for 1 hour and at 380 K (107°C) for 2 hours at a pressure of 5.5×10^5 Pa (80 psig). The total weight at installation is about 8.6 kg (19 lb). It was estimated that about 5.9 kg (13 lb) of insulation remains in the motor after firing. This is based on measured expended mass and measured nozzle erosion.

Samples of the three sections described above and of charred insulation materials taken from an engine fired at atmospheric pressure were tested in the micro-VCM test apparatus. The results of the tests, which consist of exposing the samples to a temperature of 398 K (125°C) for 24 hours and measuring the percentage total mass loss (TML) and the collected volatile condensable mass (CVCM) on a 298 K (25°C) plate, are listed in Table 1. The samples which were prepared by Thiokol Corporation for these tests have been identified by their physical appearance.

The TML's varied from 1.38 to 5.89 percent and the CVCM from 0.16 to 1.54 percent. The larger quantities were obtained for samples which had an adhesive for the bonding of the insulation to the titanium case (the samples had a commercial aluminum foil to simulate the titanium). An average of the TML results is 3.2 percent and the CVCM is about 0.64 percent. The charred material produced a 2.22-percent TML and a 0.73-percent CVCM. The basic insulation produced a 2.4-percent TML and about a 0.3-percent CVCM.

Thermogravimetric tests of the basic insulation material were also performed. The samples were heated as rapidly as possible, under vacuum, to temperatures of 398 K, 473 K, and 523 K (125°C, 200°C, and 250°C). These temperatures were then maintained for the remainder of the tests. The weight loss of the samples was measured continuously for the 24-hours duration of the test. The results are shown in

Table 1
Micro-CVCM Test Results

Material Physical Appearance	TML Percent	CVCM Percent
One Black Surface, Other Green with Adhesive, ~1.5mm Thick	3.67	0.88
One Black Surface, Other Teflon, ~1.0mm Thick	1.38	0.25
One Cloth Surface, Other Green with Adhesive, ~1.0mm Thick	5.89	1.54
Basic Insulation, Green	2.40	0.30
Charred Material from Fired Motor	2.22	0.73
Charred "Asbestos-like" Material from Fired Motor	3.68	0.16

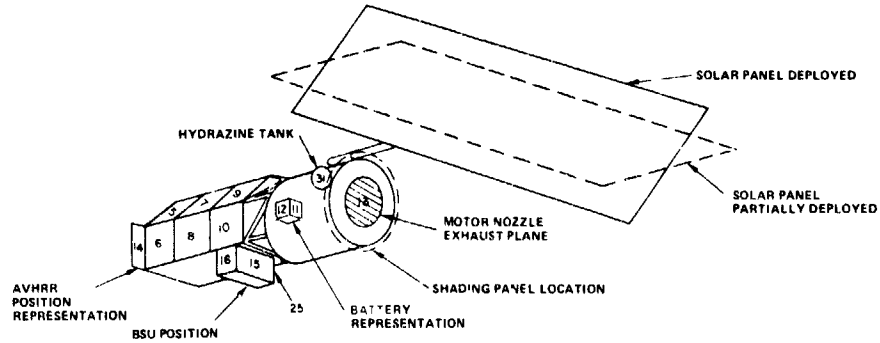

SOLAR PANEL NODES ARE 1, 2, 3, 4, 17, 18, 19, and 20 NUMBER ASSIGNMENTS VARY ACCORDING TO ORIENTATION

VIEW FACTORS (10^{-8} cm^2) MULTIPLIERS

NODE	5	6	7	8	9	10	11	14	15	16	25	31	SOLAR PANEL
NO SHADE	3 73	1 25	4 99	1 69	6 91	2 33	31 19	20 15	29 33	3 01	4 35	54 34	1068
6¼ INCH DIAMETER SHADE	3 89	1 20	4 93	1 60	6 74	2 17	15 11	19 78	20 29	2 45	2 79	23 90	1068
12 INCH DIAMETER SHADE	3 56	1 12	4 65	1 48	6 19	1 98	6 00	15 58	13 49	1 92	1 88	1 98	1068

Fig. 1—View factor nodal configuration of spacecraft

Figures 3a, 3b, 3c, and 3d. The 71.2-mg sample lost about 2 mg while at room temperature and during the 10 minutes needed to reach 473 K (200°C) (Figures 3a and 3b). At 473 K (200°C) (see Figure 3c), it lost 1.8 mg in about 1.2 hours. This loss was followed by an additional loss of 0.98 mg until that portion of the test was terminated. The total loss for the 24 hours is therefore about 6.7 percent and the long-term fraction of this may be between 1.37 and 3.9 percent. Figure 3d shows the change in weight as the material was heated (at a constant rate) above 473 K (200°C).

Figure 4 shows the accretion rates of the outgassing from a sample of the insulation held at a temperature of 473 K to 523 K (200 to 250°C) for about 4 hours as measured by two QCM's, one held at 211 K (-62°C) and the other at 296 K (+23°C). The QCM's had the same field-of-view of the source. The insulation was heated on its rear side to about 523 K (250°C) while the side facing the QCM's was 473 K (200°C). After an initially increasing rate of deposit, reaching a maximum of 440 Hz/min for the 211 K (-62°C) QCM and 170 Hz/min for the 296 K (+23°C) QCM, obtained within 8 minutes from the start, these rates decayed as shown. The rate as measured by the 296 K (+23°C) QCM dropped more rapidly than the other, indicating a depletion of the material accreting at that temperature. The total accumulation on the 211 K (-62°C) QCM was, using a sensitivity of 4.45×10^{-9} g/cm^2 Hz and taking the density of the material as 1.4 g/cm^3, 1.9×10^{-5} g/cm^2, and on the 296 K (+23°C) QCM, 4.3×10^{-6} g/cm^2, giving a ratio of about 4.4. The test, which was intended to provide a deposit of contaminant for measurement of optical degradation, was not repeated at different temperatures.

The evaporation rates at different surface temperatures, from 253 K to 300 K (-20°C to +27°C), of the material which had been deposited on the QCM at 211 K (-62°C), are shown on semilog paper in Figure 5. The rates measured for a period of 30 minutes for each temperature appear to have the same slope, indicating the material being evaporated at the various temperatures had the same properties.

On the other hand, the material component deposited on the 296 K (+23°C) QCM left this surface quite slowly as shown by the normalized curve of Figure 6. The curve covers a period of about 14 hours during which the QCM recorded continuously the mass available on its crystal.

ANALYSIS

Outgassing Components Characterization

The insulation material left in the motor following burnout has been estimated at 5.9 kg (13 lb). At the time of deployment, its temperature is about 473 K (200°C). In outgassing tests conducted at this temperature, material was deposited on a 211 K (-62°C) and a 296 K (+23°C) QCM surface as shown in Figure 4. Heating the 211 K (-62°C) surface to various

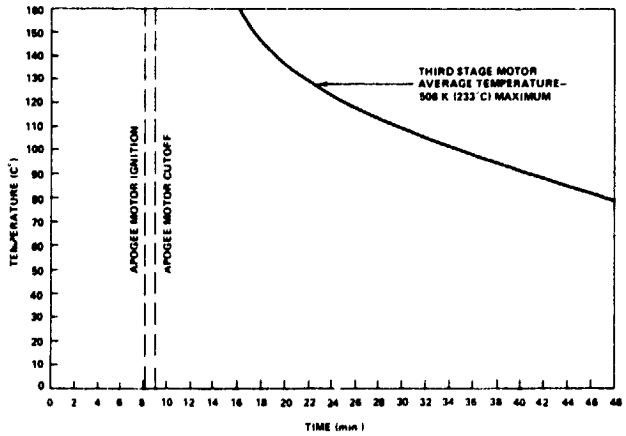

Fig. 2—Temperature history during launch

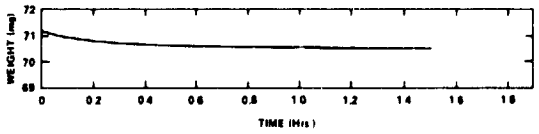

Fig. 3a—Weight loss at room temperature

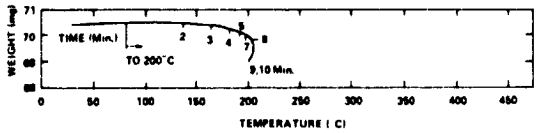

Fig. 3b—Weight loss with temperature increase to 200°C

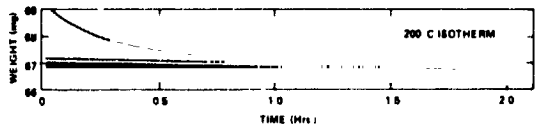

Fig. 3c—Weight loss versus time—sample at 200°C

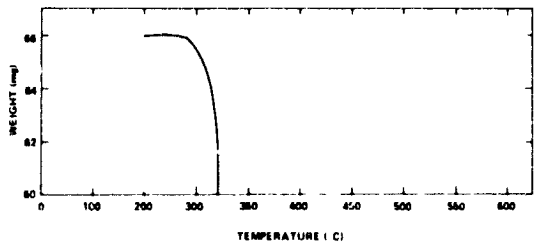

Fig. 3d—Weight change versus increase in temperature

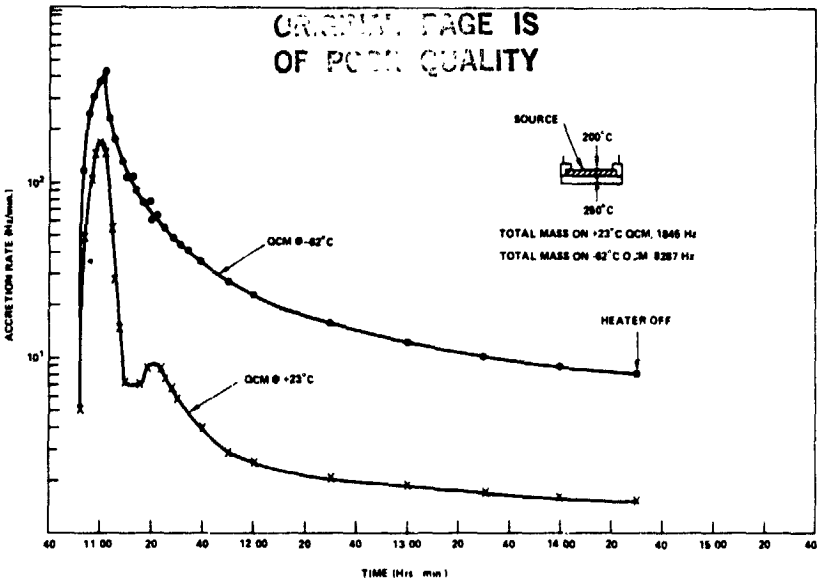

Fig. 4—Rates of deposit versus time on QCM's at -62°C and +23°C

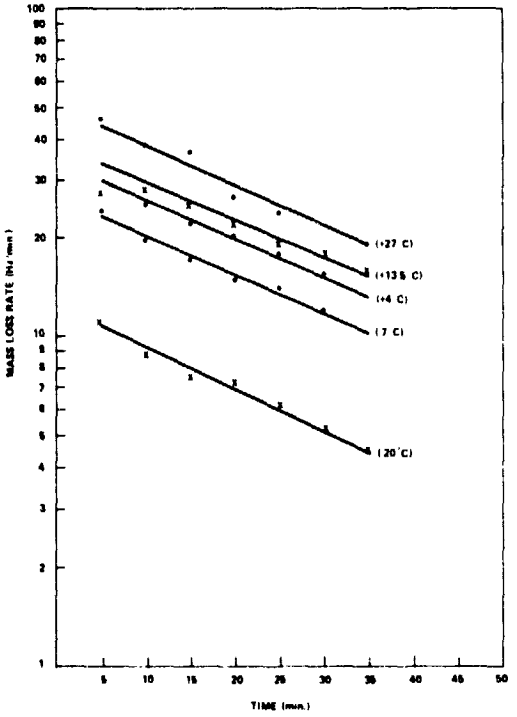

Fig. 5—Mass loss rates versus time at different temperatures of the material collected on the -62°C QCM

higher temperatures and allowing time (40 to 50 minutes) for stabilization at each plateau produced the data in Figure 5. A graph of the log of the mass loss rates versus time with temperature as a parameter resulted in a set of parallel lines. The activation energy of this material was found from the Arrhenius relation, assuming first-order reaction; this relation (Reference 2) applied at a given time and comparing rates w_1 and w_2 at two corresponding temperatures, T_1 and T_2 (in K), is:

$$\ln \frac{w_1}{w_2} = \frac{E}{R} \left(\frac{1}{T_2} - \frac{1}{T_1} \right) \tag{1}$$

where E is the activation energy for the process under consideration in calories per mole and R the gas constant in calories per mole per degree. The energy was calculated to be 5990 cal/mole. Plots of the rates versus 1/T yielded a straight line. Its slope indicated the above energy for mass loss and a confirmation of the high volatility of this material component.

In contrast, the smaller fraction of the insulation deposited on the 296 K (+23°C) surface desorbs very slowly from a surface at 295.5 K (+22.5°C) as shown in Figure 6. The depletion of this material from the surface at constant temperature is expressed by the relation (Reference 2),

$$m = m_o e^{-t/\tau} \tag{2}$$

where m_0 is the initial mass on the surface, t is time, and τ is the residence time of the molecule on that surface, i.e., the time needed for $m = m_0/e$. It is given by

$$\tau = \tau_o e^{E/RT} \tag{3}$$

where T is the surface temperature in K, and $\tau_0 \simeq 10^{-13}$ s is the average oscillation period of a surface molecule. The curve of Figure 6, when fitted to equation 2, indicated τ to be about 62.5 hours. The initial mass, m_0, was 4.28×10^{-6} g/cm^2. The activation energy for this low volatile fraction of the insulation material was then found to be E = 24.7 kcal/mole when using τ = 62.5 hours, T = 295.5 K, and R = 1.98 cal/mole K in equation 3. The residence time for this material at other temperatures can be found from equation 3, assuming that the above energy does not change appreciably with temperature. A direct relation between residence time τ_2 at temperature T_2 and τ_1 at T_1 is

$$\tau_2 = \tau_o \left(\frac{\tau_1}{\tau_o} \right)^{T_1/T_2} \tag{4}$$

where τ_o is the constant given previously. Using this expression, the time for the initial mass of deposit to become 1/e was calculated to be 16 days at 283 K (+10°C), 471 days at 263 K (-10°C), and as indicated from the test, 62.5 hours at 295.5 K (22.5°C). It is apparent that this fraction of the outgassing is of major concern for the contamination. It will remain for a long time on the surfaces on which it deposits. During this stay, it can be polymerized by radiation and may remain permanently on the surfaces. It has been estimated from the considerations which follow that its fraction of the outgassing is about 1.4 percent, corresponding to about 82 g of the total 5.9 kg of material remaining in the engine at burnout. These considerations form the basis for this estimate. The CVCM at 398 K (125°C) for the charred material is 0.73 percent and the average for all materials configurations is 0.64 percent. If these results are modified by the 0.54 view factor of the collector plate to the exit flow port of the VCM apparatus (Reference 3), the actual condensables on the 298 K (25°C) collector are 1.2 to 1.35 percent of the sample. The TG test at 473 K (200°C) showed a long-term mass loss which corresponds to 1.37 percent of the total.

Outgassing Flow from the Motor

The TG test of the sample at 473 K (200°C) showed that an initial exponentially decaying mass loss occurred from the time 473 K (200°C) was obtained and that a condition of a small, quasi-steady mass loss was reached. That mass loss was L = 1.8 mg obtained in a period of Δt = 1.2 hours. The sample mass when 473 K (200°C) was reached was the initial mass, W_o = 71.2 mg less the losses, W_t = 1.2 mg, to get to the temperature and the loss, W_r = 0.8 mg, at room temperature. The flow rate from the motor at 473 K (200°C) can be estimated applying these test results to the VCM fraction, 1.4 percent, of the total mass of the insulation remaining after burnout, W_i = 5.9 kg, as follows:

$$\dot{m}_i = \frac{L}{\Delta t} \frac{[CVCM \cdot W_i]}{[W_o - (W_t + W_r)]} = 1.77 \text{ g/hr} = 2.96 \times 10^{-2} \text{ g/min} \quad (5)$$

An alternate estimate can be obtained from the initial, maximum rate of insulation depositing on the 211 K (-62°C) QCM. This rate, $\Delta f/\Delta t$ = 440 Hz/min as shown in Figure 4, must be modified to get the rate of outgassing at the sample source. The parameters for this modification are: the view factor between source and QCM, $F = 1.07 \times 10^{-4}$, for the test arrangement; the area A_c = 0.317 cm^2 of the QCM crystal detecting surface; the area of the insulation sample A_s = 20.26 cm^2; the density ρc = 2.7 g/cm^3 of the quartz crystal and ρ = 1.4 g/cm^3, the experimentally measured density of the material. The rate of outgassing per unit area, ϕ, for the material at 473 K (200°C) is then:

$$\phi = \frac{A_c}{A_s F}\left(\frac{\Delta f}{\Delta t}\right)\left(\frac{\nu}{\rho_c}\right) \quad k = 2.5 \times 10^{-6}\ g/cm^2/s = 1.5 \times 10^{-4}\ g/cm^2/min \quad (6)$$

where $k = 4.45 \times 10^{-9}$ g/cm^2 -Hz is the mass constant for the 10 MHz QCM. For a steady-state pressure-controlled outgassing, the flux inside the motor is constant and the flow from the motor which has a throat area A = 55 cm^2 is

$$\dot{m} = \phi A = 8.25 \times 10^{-3}\ g/min$$

The rate $\dot{m} = 2.96 \times 10^{-2}$ g/min, obtained from the TG test, is 3.7 times larger than this and it has been used as a measure of the motor flow rate when the insulation is at 473 K (200°C). One can also obtain the flow at 473 K (200°C) starting from the data at 495.5 K (22.5°C) in Figure 6. In fact, the initial rate at 295.5 K (22.5°C), which is 1.14×10^{-9} g/cm^2/min when modified with the residence times (62.5 hours) at 295.5 K (22.5°C) and 8.12×10^{-6} hours at 473 K (200°C), indicates a rate of 8.75×10^{-3} g/cm^2/min and a corresponding flow of 4.85×10^{-1} g/min. This flow is about 16 times higher than the one being used. However, the TG value was used because of its direct determination from a test at 473 K (200°C) and in view of the many assumptions needed in the large extrapolation from 295.5 K (22.5°C) to 473 K (200°C).

The change in outgassing rate, due to the decreasing temperature of the insulation with time, has been estimated using the activation energy derived previously, under the assumption that it is valid at those temperatures. Equation 2, differentiated with respect to time, gives the rate as a function of time with the temperature as a parameter. The ratio of the initial rates for the same material at temperatures T_1 and T_2 is

$$\frac{\dot{m}_1}{\dot{m}_2} = \frac{\tau_2}{\tau_1} = \exp\frac{E}{R}\left(\frac{1}{T_2} - \frac{1}{T_1}\right) = \tau_0 \frac{\left(\frac{\tau_1}{\tau_0}\right)^{T_1/T_2}}{\tau_1} \quad (7)$$

where the various forms of the equations are in accordance to equations 3 and 4. The rates versus temperature, based on E = 24.7 kcal/mole and calculated using this relationship, are shown in Figure 7.

Contaminant Deposit on Solar Cells and Hydrazine Tanks

The contaminant accretion rate ($\Delta M/\Delta t$, where ΔM is the difference in mass over the time period Δt) on a spacecraft surface of temperature T = C, is the product of the flow from the motor, times the view factor

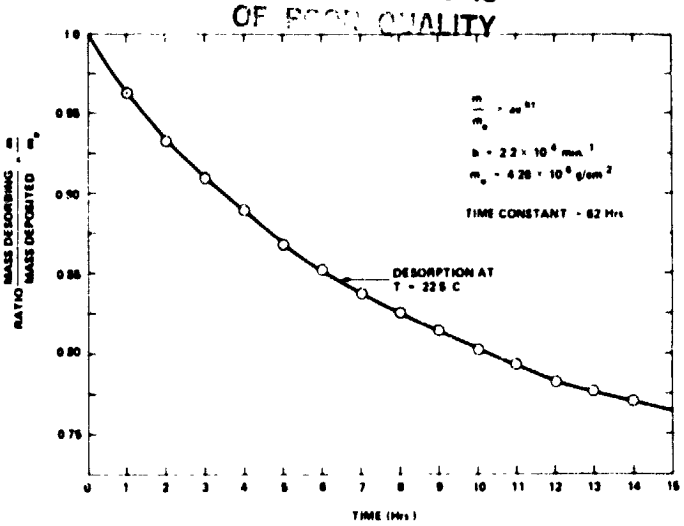

Fig. 6—Mass desorbing from a QCM at 22.5°C versus time

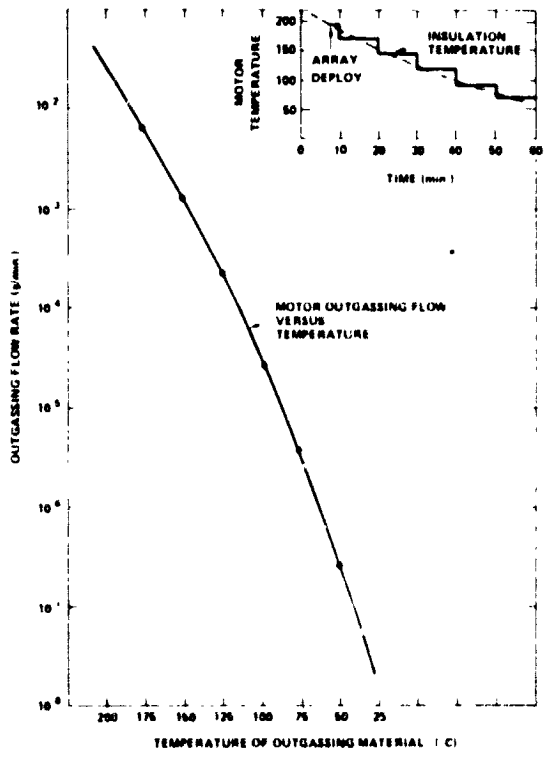

Fig. 7—Outgassing rates versus motor temperatures

ψ and a sticking coefficient σ, so that

$$\left.\frac{\Delta M}{\Delta t}\right|_{r=c} = \dot{m}(t)\,\psi\sigma \qquad (8)$$

The rate, $\dot{m}(t)$, varies with the motor temperature as shown in Figure 7. Since the temperature decreases with time, $\dot{m}$ is a function of time. For the calculation made here, the rates have been assumed to change every 10 minutes by an amount corresponding to a 25 K drop. The rates have not been reduced to account for material depletion. This is a conservative assumption, also justifiable, on account of the relatively short time (about 80 minutes) for the insulation material to acquire a temperature of about 298 K (25°C) and a corresponding outgassing rate several orders of magnitudes lower than that at 473 K (200°C).

The view factor multiplier, ψ (cm^{-2}), as defined here, expresses the fraction of the total material from the motor which impinges on a unit area of the spacecraft surface under consideration. The view factor multipliers for the numbered surfaces are indicated in the tabulation in Figure 1. View factor multipliers for the same surfaces, but modified by different diameters of proposed baffle rings around the motor, have been indicated for comparison. These baffle rings were suggested as a possible modification if the deposits were found to be too large. These view factor multipliers are based on the sources being diffuse and on averaging for the array rotation. The conventional view factors for the total area viewing the flow from the engine were calculated using Reference 4. The factor, $\psi = 1.06 \times 10^{-5}\ cm^{-2}$ applies to the solar cells surface, which will be exposed for 2 minutes during the array deployment. The next largest value, $\psi = 5.4 \times 10^{-7}$ cm^{-2}, applies to the hydrazine tanks. The deposits on the tanks will be the largest for any other critical surface of the spacecraft. Therefore, calculations for these were used as a conservative estimate of contamination on other, more removed surfaces from the motor.

The sticking coefficient, σ, is the fraction of the impinging contaminant which remains on the surface. It has been taken as unity for the deposits on the cells and tanks. The temperatures of these are estimated to be 243 K (-30°C) for the cells and 273 K to 263 K (0 to -10 C) for the insulation on the tanks at the time of and several hours after deployment. At these temperatures, the stay times of the molecules of this high activation energy material are very long (471 days at 263 K (-10°C)) and the rates of evaporation are less than $10^{-12}\ g/cm^{-2}/min^{-1}$. Therefore, the 100-percent sticking is not only conservative, but is based on justifiable grounds. However, for reasons of conservatism, it was assumed that 10 percent of the total contaminant would reach the

tanks during the 2 minutes of solar array deployment. After these 2 minutes, the solar array is fully deployed and the opposite side of the cells, which now views the spacecraft, is taken as a 100-percent diffuse reflector.

The deposit, ΔM, on the surface for a time, Δt, while the temperature is constant, is

$$\Delta M = \sigma \psi \left[\dot{m} \Delta t\right]_{T=C} \tag{9}$$

The total deposit, M, will be the summation of these elemental deposits at constant temperatures, i.e.,

$$M = \sum \Delta M = \sum \sigma \psi \left[\dot{m} \Delta t\right]_{T=C} \tag{10}$$

The rates and deposits on the solar cells and tank insulation have been calculated using these expressions. Table 2 shows a sample of the calculations and Figure 8 the deposits on the cells and insulation as a function of deployment time. For a deployment 8 minutes after motor burnout, which is probably the earliest deployment, the deposit on the cells is calculated at 6.2×10^{-7} g/cm^2 and on the tanks at 4.6×10^{-8} g/cm^2. These masses correspond to thicknesses of about 43 Å and 3.5 Å when the measured material density of 1.4 g/cm^3 is used. The deposits decrease by a half decade or more for every 10 minutes' delay in deployment.

CONTAMINANT-INDUCED SURFACE DEGRADATION

Test Set-Up and Instruments

The test for the measurement of surface degradation was run in a liquid nitrogen-shrouded vacuum chamber at a pressure of 5×10^{-6} torr. The layout of the thermal test samples in the X-25L solar simulator beam is shown in Figure 9. A QCM was positioned in the beam and another located outside the beam. The contaminant source was located beneath the quartz entrance window with its normal towards the sample plane. A radiometer for monitoring the output of the solar simulator was located externally to the vacuum chamber. A specially built system for recording QCM data and for thermally controlling the QCM was used for this test. The QCM's (which were the commercially available Celesco Model 700) were mounted inside a separate liquid nitrogen-cooled shroud. Their temperatures can be maintained at any desired temperature above 90 K by balancing the electrical power into a resistance heater on the QCM holder against the heat loss to the shroud. The sensing heads of these QCM's contain a demountable crystal assembly, a mixer/oscillator circuit, a stainless steel base in which these components are mounted, and a stainless steel cover for the crystal

Deposits on Solar Cells and Hydrazine Tank Insulation
for Array Deployment 8 Minutes after Burn and 2 Minutes of Solar Cells Exposure

Time from Motor Shutdown	Source Temperature	Outgassing of Motor	Solar Cells		Hydrazine Tank	
			Impinging Rates	Deposits	Impinging Rates	Deposits
min	°C	g/min	g/min/cm^2	g/cm^2	g/min/cm^2	g/cm^2
0 - 8	-	-	-	-	*	-
8 - 10	200	2.96×10^{-2}	3.16×10^{-7}	6.32×10^{-7}	1.60×10^{-9}	3.20×10^{-9}
10 - 20	175	6.34×10^{-3}	-	-	3.44×10^{-9}	2.44×10^{-8}
20 - 30	150	1.26×10^{-3}	-	-	6.84×10^{-10}	6.84×10^{-9}
30 - 40	125	2.11×10^{-4}	-	-	1.16×10^{-10}	1.16×10^{-9}
40 - 50	100	2.53×10^{-5}	-	-	1.37×10^{-11}	1.37×10^{-10}
50 - 60	75	4.22×10^{-6}	-	-	2.29×10^{-12}	2.29×10^{-11}
60 - 70	50	2.11×10^{-7}	-	-	1.14×10^{-13}	1.14×10^{-12}
70 - 80	25	9.51×10^{-9}	-	-	5.16×10^{-15}	5.16×10^{-14}
80 - 90	~25	$<9.51 \times 10^{-9}$	-	-	$<5.16 \times 10^{-15}$	$<5.16 \times 10^{-14}$
				$\Sigma = 6.32 \times 10^{-7}$ (43 Å)†		$\Sigma = 4.56 \times 10^{-8}$ (3.5 Å)†

Notes:

*Assumes 10 percent reflection from array.

†Contaminant density 1.4 g/cm^3.

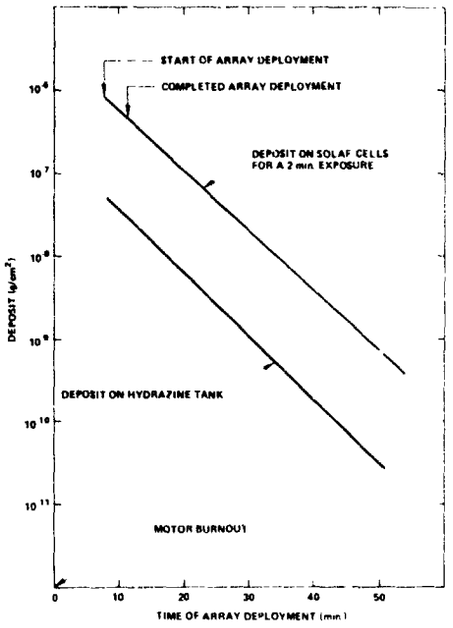

Fig. 8—Material deposit on solar cells and hydrazine tanks as a function of solar array deployment

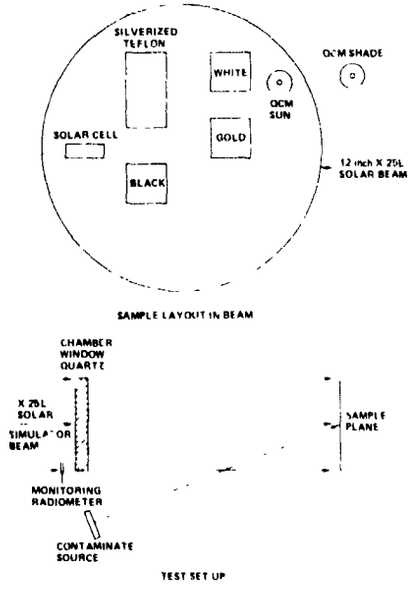

Fig. 9—Layout of thermal test samples in X-25L solar simulator beam

assembly. The crystal assembly contains the sensing and reference crystals and a platinum resistance thermometer between the two crystals. The AT-cut crystals are about 1.27 cm (0.5 inch) in diameter and 0.0152 cm (0.006 inch) thick, with a 10 MHz resonant frequency. The electrodes, serving as the contaminant deposit area, are aluminum with a 0.635-cm (0.25-inch) diameter.

The Deposit of Contaminants on the QCM and Sample Surfaces

The motor insulation sample used during the test was sandwiched between two 10-cm x 10-cm (4-inch x 4-inch) aluminum plates with a 5-cm (2-inch) diameter hole on the forward plate. Two 50 W heaters were bonded on the rear panel in order to drive the temperature of the source to 523 K (250°C). One thermocouple was centered on the insulation in the 5-cm (2-inch) diameter hole while another was located about 2.5 cm (1 inch) from the edge of the holder.

The physical appearance of the forward facing side of the insulation remained unchanged before and after the test, i.e., a relatively shiny black. The major change occurred in the material bonded between the aluminum foil backing and the rubber insulation. Initially, the material beneath the aluminum foil was shiny green and relatively flexible. At the test completion, this layer of material had become brittle and changed to a dull black. Heating schedules of the source had been intended to produce deposits corresponding to about 10^3, 5×10^3, and 1×10^4 Hz on the QCM. It was not possible, however, to produce deposits greater than about 4400 Hz.

The accretion rates on the QCM's which were aligned to face the source and were held at 213 K are shown in Figure 10. It was necessary to continuously increase the contaminant source temperature in order to achieve a reasonable deposition rate on the QCM's. During the last maximum source temperature, the QCM accretion rate decreased rapidly even with increasing source temperature indicating depletion of outgassing products. The total amount of time the contaminant source was above 273 K was 9-3/4 hours and the total deposition on the QCM was 4.05×10^{-5} g/cm^2.

Test Technique for α/ϵ Determination

The thermal method to measure the integrated absorptance, α, and thermal emittance, ϵ, by the rate of temperature change during heating with the X-25L solar simulator on/off, was employed. The radiant intensity of the solar simulator was continuously monitored by a radiometer during the heat-up phase of this procedure. The data reduction procedure was essentially that documented in Reference 5.

RESULTS

The silverized Teflon sample was black on the reverse side and edges and the data presented is for this configuration. Figure 11 shows the degradation of the sample α and ϵ versus mass loading as indicated by the QCM. The sample ϵ was degraded at all three mass loadings, whereas the α was not significantly perturbed until after 2.1×10^{-5} g/cm^2 was deposited. The resultant α/ϵ ratio, which is also given in Table 3, is thus driven by the decreasing ϵ values. The visual appearance of the sample after the final contaminant loading was "hazy" and fringes could be seen when the Sun gun was rotated with respect to the sample. A reflectance measurement was made (using a Beckman DK-2A recording spectrophotometer) before and after (2.1×10^{-5} g/cm^2) on the sample with the results given in Figure 12. No data are given beyond 600 nm as there was no significant change in the reflectance. The spectral region below 400 nm displayed the most significant decrease in reflectance due to the contaminant film.

The white sample α and ϵ values exhibited the same trend as the silverized Teflon as shown in Table 3.

The evaporated gold sample α changed at all of the three levels of contaminant mass loading. The ϵ for gold could not be determined because black stripes, which were included to prevent excessive temperatures which would result with an all gold sample, dominate the thermal ϵ characteristic of the sample.

The solar cell output as a function of mass loading is given in Figure 13. The solar cell was at 248 K (-25°C) during the contaminant loading periods with the X-25L solar simulator on. The ratio of solar cell output to solar simulator monitoring radiometer is plotted to account for any fluctuations which occur in the X-25L simulator. The data are a composite of two separate mass loadings with the cell being cleaned between runs. With the QCM mass loading above 3.4×10^{-6} g/cm^2, the solar cell indicated no further decrease in output, even at the maximum loading of 3.0×10^{-5} g/cm^2. The reason for this characteristic is not known.

CONCLUSIONS

A deposit of 6.2×10^{-7} g/cm^2 on the solar cells corresponding to a thickness of about 43 Å which was calculated for the earliest solar array deployment, will not affect to a detectable degree, the performance of the solar cells. In fact, according to the degradation tests, a deposit, an order of magnitude higher than that calculated, produces a 4-percent degradation in cells' performance.

Similarly, the accretion of about 5×10^{-8} g/cm^2 (3 to 4 Å) on the silver-coated Teflon insulation of the hydrazine tank, is too small to

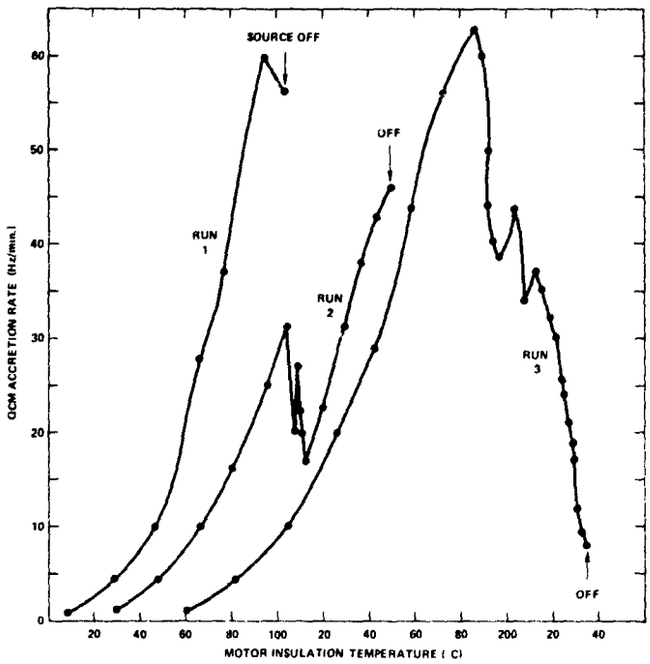

Fig. 10—QCM accretion rate versus motor insulation temperature

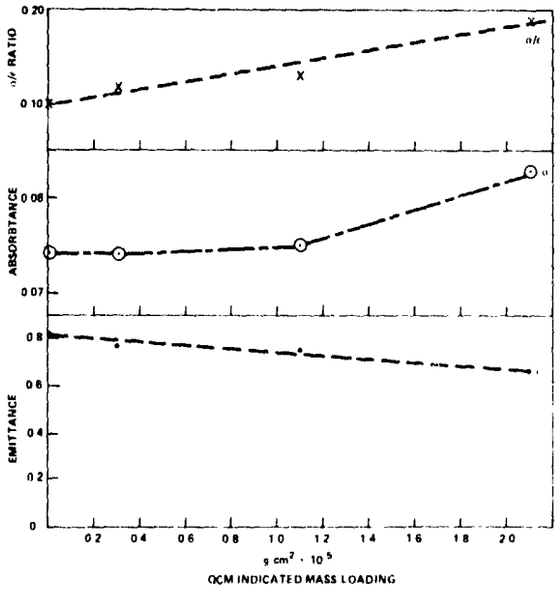

Fig. 11—Silverized Teflon absorptance and emittance versus contaminant mass

Table 3
Absorptance and Emittance
versus
QCM Indicated Mass Loading

QCM Indicated Mass Loading g/cm^2	White				Silverized Teflon (Black on Reverse Side)*				Gold (Black Stripes on Reverse Side)*		
	α	ϵ	α/ϵ	Temp.† °C	α	ϵ	α/ϵ	Temp.† °C	α	ϵ	Temp.† °C
Clean	0.14	0.90	0.16	-54.7	0.074	0.82	0.10	-74	0.21	0.47	-6.8
3.0×10^{-6}	0.14	0.86	0.16	-52.5	0.074	0.77	0.12	-72	0.24	0.47	+3.3
1.1×10^{-5}	0.14	0.79	0.18	-48	0.075	0.74	0.13	-70	0.26	0.47	+8.7
2.1×10^{-5}	0.16	0.70	0.23	-36	0.67	0.67	0.20	-62	-	-	-

Notes:

*Black treatment used for temperature control.

†Temperature at stabilization with Sun on.

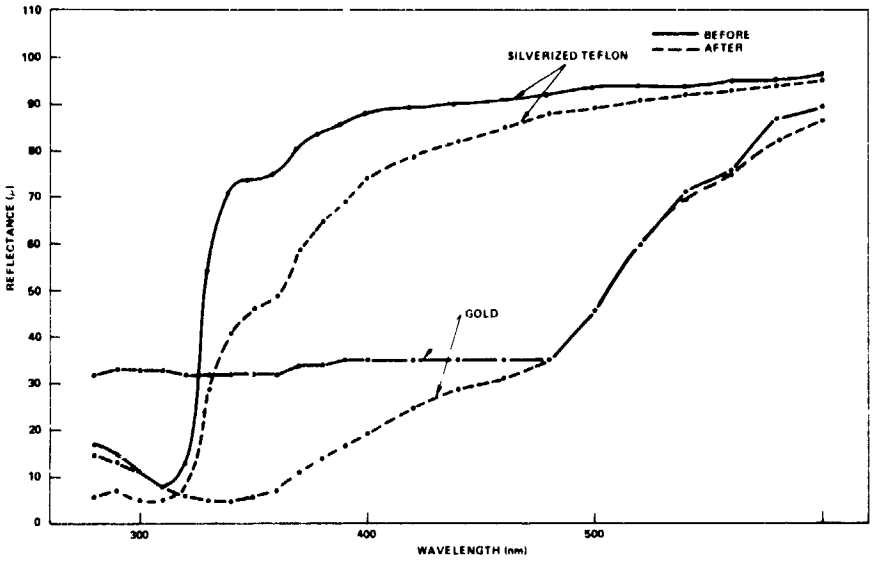

Fig. 12—Reflectance change of silverized Teflon and gold

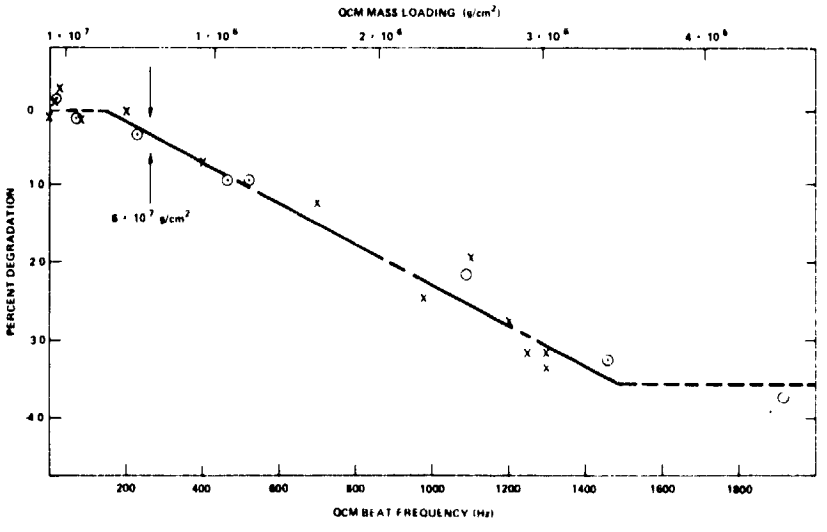

Fig. 13—Solar cell versus QCM mass loading

cause sensible change in the α/ϵ properties of the surface. The degradation test showed an α/ϵ change from 0.10 to 0.12 when a film of 3×10^{-6} g/cm^2, about 220 Å thick, was added to the clean surface. Degradation data as a function of mass deposits have been provided for the above surfaces, and for a white surface and a gold surface.

In conclusion, these degradation tests indicate that the calculated deposits would have to be one or two orders of magnitude higher to produce sensible effects on the thermal optical properties of the surfaces on which they will deposit. On the other hand, no estimate was possible on the size distribution, quantities, and velocities of particulates ejected by the motor 8 minutes after its firing, without actual engine firing and statistical measurements. If a number of particulates deposited on surfaces, they would be centers of scattering. Those orbiting for a time with the spacecraft would be sporadic sources of interference with radiation observations.

ACKNOWLEDGMENTS

The authors thank T. J. Jarrell and A. C. Darrah for computing the view factors, R. Marriott for the VCM data, F. C. Gross for the TG data, B. Paxson and A. R. Winker for the test set-up and operations, and E. Kunz of Thiokol Corporation for providing motor samples and related data.

REFERENCES

1. Brooksbank, R. M., "Qualification Test of a Thiokol TE-M-364-15 Rocket Motor at Simulated Altitude Conditions, "AEDC-TR-74-27. Rev., May 1974.

2. Santeler, D. J., Holkeboer, D. H., Jones, D. W., and Pagano F., "Vacuum Technology and Space Simulation," NASA SP-105, pp. 184-198.

3. Scialdone, J. J., "An Equivalent Energy for the Outgassing of Space Materials," NASA TN-8294, August 1976.

4. Jackson, C. E., Jr. and Puccinelli, E. F., "Viewfactor Computer Program (VIEW)," NASA Tech Brief B-75-10032, April 1975.

5. "Measurement of Thermal Radiation Properties of Solids," Richmond, J. C., ed., NASA SP-31, pp. 89-90.